

Tonnage Uncertainty Assessment of Vein-Type Deposits Using Distance Functions and Location-Dependent Correlograms

David F. Machuca-Mory, Michael J. Munroe and Clayton V. Deutsch

Modelling the geometry of a vein is a crucial step in resources estimation. The resulting models are used as mineralization domain boundaries and have a direct impact on the tonnage of estimated resources. Deterministic models are often built using time consuming wireframing techniques usually based on hand interpretation of the drillhole intercepts. Another approach consists in coding the drillhole samples by a function of their distance to the veins contacts. The coding is subsequently used for modelling the vein contacts away from drillholes. This is a more efficient approach and is able to provide a measure of tonnage uncertainty. The use of location-dependent variograms improves the modelling by incorporating local changes in the anisotropy of the vein structure. This combined approach results in more realistic vein models, particularly when the geometry of the vein has been altered by folding, shearing and other structural processes. This numerical approach is illustrated on a realistic case study.

Introduction

The geostatistical techniques currently used in mineral resources evaluation require the assumption of some kind of stationarity. This assumption can be understood as the decision of pooling data deemed statistically and geologically homogeneous. Since it is rare a deposit containing a single geological unit with homogeneous mineralization, it is very often necessary to delimit domains where samples can be reasonably assumed to belong to the same population. Ignoring the differences of the various populations present in a deposit by considering them as homogeneous may lead to biased estimates. This is particularly critic in vein deposit modelling, where samples taken within the vein structure usually exhibit much higher grades than those taken from the wall rock.

Three dimensional geological modelling has been one of the most popular applications of mining software since its use became widespread in the mining industry from the late eighties and through the nineties (Gibbs, 1990). Since then and until now, the most popular technique for 3-D domain modeling is the wireframe interpolation of the interpreted geological contacts in level plans and cross sections (Houlding, 2000, p. 62) Although several algorithms have been implemented in commercial software for facilitating this procedure, this remains a highly demanding task in terms of professional time. Moreover, the resulting deterministic wireframe model is highly dependent of the geologist's particular interpretation and biases can be introduced without providing enough flexibility to consider alternative scenarios. An alternative technique that is becoming increasingly popular is the rapid geological modeling based on radial basis functions (RBF) (Cowan, Beatson, Fright, McLennan, & Mitchell, 2002; Cowan, et al., 2003). The RBF function is applied for the interpolation of the isosurface that delimits positive distances outside the geological unit from the negative distances within it. This coding of the available data according to their relative distance to the contact is achieved using a volume function. The requirement of geologic by hand interpretation is minimized or eliminated. Moreover, the versatility and speed offered by this technology allows the construction of multiple alternative models by changing the parameters of the radial basis function. However, the RBF based rapid geological modeling does not offer a complete assessment of the vein volume uncertainty.

The use of simulation techniques, such as the indicator P-field Simulation (Srivastava, 2005) as an alternative to the deterministic modeling of tabular ore bodies has been proposed. The simulation approach can provide a rigorous assessment of the vein volume uncertainty. However, this requires the generation of multiple realizations, which may be highly demanding in computer resources.

The alternative approach presented in this paper is based in a similar coding of the samples according to their distances to the contact as the used by the rapid geological modeling. But instead of interpolating the distances using a RBF, simple kriging is used. Uncertainty assessment is performed by calibrating the distance function parameters that control the bias and uncertainty range of the vein contact isosurface. The theoretical framework of the distance function and its parameters for uncertainty assessment is explained in the next section. The following section presents the methodology for obtaining location-

dependent measures of spatial continuity in order to depict local changes in the vein geometry, and for incorporating them in the interpolation of the distance function. The application of this combined methodology is illustrated with data from a copper deposit and compared with the deterministic volume of a corresponding wireframe model.

Distance Function Methodology

A detailed discussion of volume modelling using distance functions has been presented by Munroe and Deutsch (2008a). A brief review of the most relevant aspects of this methodology is given next.

The distance function (DF) used for boundary modelling is based on the Euclidean distance between a sample and the nearest sample with a different indicator in the same drillhole. This requires a drillhole database with intervals numerically coded according the domains they intercept. Basically this coding is a binary categorical indicator of the form (Deutsch & Journel, 1998, p. 46):

$$VI(\mathbf{u}_\alpha) = \begin{cases} 1, & \text{if } \mathbf{u}_\alpha \text{ is located within the vein} \\ 0, & \text{otherwise} \end{cases} \tag{1}$$

Where \mathbf{u}_α is the sample location. The DF is defined as positive outside the domain of interest and negative within it. It can be suited to take into account the geometric anisotropy defined by the major directions of continuity parallel to the strike and the dip of the tabular structure, such as:

$$DF(\mathbf{u}_\alpha) = \sqrt{\left(\frac{dx'}{hx'}\right)^2 + \left(\frac{dy'}{hy'}\right)^2 + \left(\frac{dz'}{hz'}\right)^2} \tag{2}$$

Where dx' , dy' , and dz' are the separation between the sample location \mathbf{u}_α and the closest change in the VI function. Whereas hx' , hy' , and hz' are the anisotropic radius defined along the rotated axis x' , parallel to the global vein strike, y' , parallel to the global vein dip and z' , perpendicular to the plan defined by the two first axis.

The DF values cannot be regarded as realizations of a Stationary Random Function, thus, their uncertainty cannot be assessed by rigorous probabilistic models (McLennan, 2007, pp. 4-15). Instead, a less formal approach based on the extent of the uncertainty and the bias of the DF is proposed. Under this approach the DF in (2) is modified by two parameters, C and β . The first controls the width of uncertainty (see Figure 1) and the second acts as a bias correction constant. Thus, the modified DF is defined as:

$$DF_{\text{mod}}(\mathbf{u}_\alpha) = \begin{cases} (DF(\mathbf{u}_\alpha) + C) / \beta & \text{if } VI(\mathbf{u}_\alpha) = 0 \\ (DF(\mathbf{u}_\alpha) + C) \cdot \beta & \text{if } VI(\mathbf{u}_\alpha) = 1 \end{cases} \tag{3}$$

The parameter C is a function of the drilling separation (DS) and it is calculated as:

$$C = \frac{1}{2} c \cdot DS \quad \text{with } c \in [0,1] \tag{4}$$

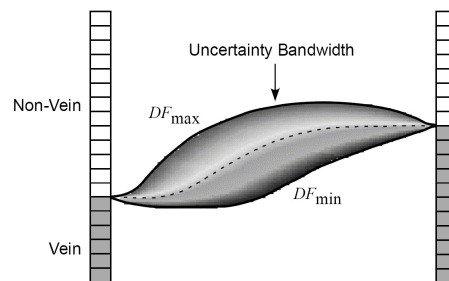


Figure 1: Schema of smooth uncertainty boundaries between drill holes.

For $c = 0$ the uncertainty bandwidth has zero thickness, therefore no uncertainty is considered. If $c = 1$ the uncertainty bandwidth is as thick as the drill hole separation. While C controls the width of the uncertainty region, β defines the position of the uncertainty bandwidth centre. If β increases this central surface, which correspond to the iso-zero surface, expands (see Figure 2). The C and β parameter values are chosen either by empirical selection, partial calibration or full calibration. The empirical selection of the parameters is done on the basis of expert knowledge. In partial calibration, the C parameter is chosen

in order to produce a reasonable uncertainty bandwidth. Whereas, for choosing the β parameter, the $p50$ envelopes of different models resulting from the interpolation of the DF values are compared with a deterministic model of the ore body. If the deterministic model is deemed unreliable or biased, the proportions vein/waste of the DF models can be compared with the equivalent proportion in declustered data. The β value chosen is such that minimizes the bias between the interpolated models and the deterministic solid or the data proportions.

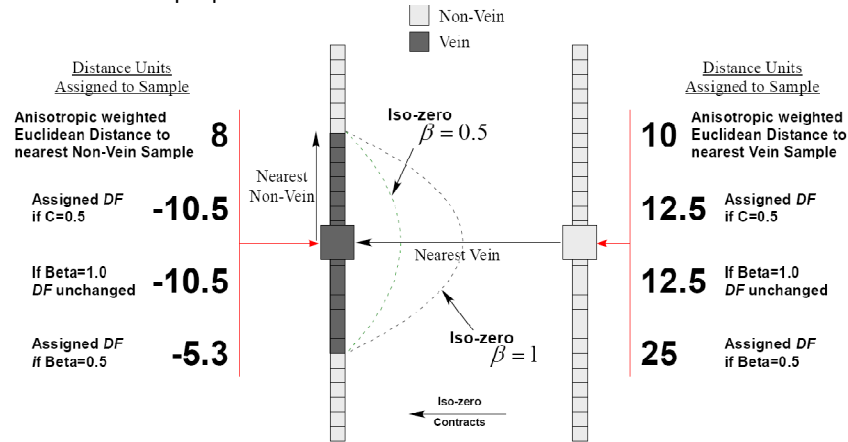


Figure 2: Schema showing the effect of β parameter in the iso-zero surface.

Full calibration requires the comparison of the interpolated model with reference stochastic model produced using geostatistical simulation methods. Recurring to partial calibration or the arbitrary selection of the DF parameters does not allow assessing the volume uncertainty as rigorously as when full calibration is performed. However, full calibration requires the extra work of building the stochastic reference models by a simulation method and using them for iteratively comparing the DF models built using different values of C and β until achieving unbiasedness and fair uncertainty. A detailed discussion on the full calibration of these parameters is given in “Full Calibration of C and Beta in the Framework of Vein-type Deposit Tonnage Uncertainty” (Munroe & Deutsch, 2008b). Full calibration is recommended only as an eventual check of the distance function uncertainty intervals in relation to those produced by stochastic simulation methods.

The interpolation of the DF values is performed using simple kriging on a regular grid. In order to account for local changes in the ore body geometry a locally stationary simple kriging based on location-dependent correlograms can be used. This methodology is explained in the next session. On the gridded distances model the inner and outer limits of the uncertainty bandwidth, DF_{min} and DF_{max} , respectively, define the next range:

$$[DF_{min}, DF_{max}] = \left[-\frac{1}{2} C \cdot DS \cdot \beta, \frac{1}{2} \frac{C \cdot DS}{\beta} \right] \quad (5)$$

The interpolated distances, DF^* , are then regularized by these limits and their corresponding p-value or probability value is obtained from:

$$p = \frac{DF^* - DF_{min}}{DF_{max} - DF_{min}} \quad (6)$$

If $p > 1$ the node is outside the vein, while if $p < 0$, it is classified as inside the ore body.

Location-dependent Correlograms

2-point statistics such as the Location-dependent measures of spatial continuity can be obtained by weighting the sample pairs inversely proportional to their distance to a reference point (Machuca-Mory & Deutsch, 2008). These weights are obtained from a smoothly decaying distance function, such as the Gaussian kernel:

$$\omega_{GK}(\mathbf{u}_\alpha; \mathbf{o}) = \frac{\varepsilon + \exp\left(-\frac{(d(\mathbf{u}_\alpha; \mathbf{o}))^2}{2s^2}\right)}{n\varepsilon + \sum_{\alpha=1}^n \exp\left(-\frac{(d(\mathbf{u}_\alpha; \mathbf{o}))^2}{2s^2}\right)} \quad (7)$$

Where $d(\mathbf{u}_\alpha; \mathbf{o})$ is the distance between the sample location \mathbf{u}_α and a reference point \mathbf{o} , s is the Gaussian Kernel bandwidth or standard deviation, and ε is a small constant that avoids computational problems when $d(\mathbf{u}_\alpha; \mathbf{o})$ is very large. The Kernel Parameters must be chosen in order to allow the local statistics to reflect the local variations without overfitting, nor oversmoothing. A rule of thumb is to choose the bandwidth between 1 and two times the average sample spacing.

In the calculation of location-dependent measures of spatial continuity the individual weights assigned to each sample are combined as geometric or arithmetic averages of pair weights. By instance, for the vein indicator in (1), the experimental location-dependent indicator covariance can be calculated as:

$$C_{VI}(\mathbf{h}; \mathbf{o}) = \frac{\sum_{\alpha=1}^{N(\mathbf{h})} \omega(\mathbf{u}_\alpha, \mathbf{u}_\alpha + \mathbf{h}; \mathbf{o}) \cdot VI(\mathbf{u}_\alpha) \cdot VI(\mathbf{u}_\alpha + \mathbf{h})}{\sum_{\alpha=1}^{N(\mathbf{h})} \omega(\mathbf{u}_\alpha, \mathbf{u}_\alpha + \mathbf{h}; \mathbf{o})} - F_{VI, -\mathbf{h}}(\mathbf{o}) \cdot F_{VI, +\mathbf{h}}(\mathbf{o}) \quad (8)$$

Where $\omega(\mathbf{u}_\alpha, \mathbf{u}_\alpha + \mathbf{h}; \mathbf{o})$ are the pair weights. The local tail and head vein proportions are obtained:

$$F_{VI, -\mathbf{h}}(s_k; \mathbf{o}) = \sum_{\alpha=1}^{N(\mathbf{h})} \omega(\mathbf{u}_\alpha, \mathbf{u}_\alpha + \mathbf{h}; \mathbf{o}) \cdot VI(\mathbf{u}_\alpha; s_k) , \quad (9)$$

$$F_{VI, +\mathbf{h}}(s_k; \mathbf{o}) = \sum_{\alpha=1}^{N(\mathbf{h})} \omega(\mathbf{u}_\alpha, \mathbf{u}_\alpha + \mathbf{h}; \mathbf{o}) \cdot VI(\mathbf{u}_\alpha + \mathbf{h}; s_k)$$

And the experimental location-dependent indicator correlogram is calculated as:

$$\rho_{VI}(\mathbf{h}; \mathbf{o}) = \frac{C_{VI}(\mathbf{h}; \mathbf{o})}{\sqrt{\sigma_{VI, -\mathbf{h}}^2(\mathbf{o}) \cdot \sigma_{VI, +\mathbf{h}}^2(\mathbf{o})}} \in [-1, +1] \quad (10)$$

With the indicator tail and head variances obtained from:

$$\begin{aligned} \sigma_{-\mathbf{h}}^2(s_k; \mathbf{o}) &= F_{-\mathbf{h}}(s_k; \mathbf{o}) [1 - F_{-\mathbf{h}}(s_k; \mathbf{o})] \\ \sigma_{+\mathbf{h}}^2(s_k; \mathbf{o}) &= F_{+\mathbf{h}}(s_k; \mathbf{o}) [1 - F_{+\mathbf{h}}(s_k; \mathbf{o})] \end{aligned} \quad (11)$$

In practice the location-dependent correlogram is preferred over the location-dependent covariance, since the first is more stable and easier to interpret. Strictly, the experimental local measures of spatial continuity should be calculated and modelled at every location. However, it is preferred do so for a limited number of reference points, \mathbf{o} . This facilitates the checking of the semiautomating fitting of local experimental correlograms and speeds up the process. The parameters of the fitted variogram models are subsequently interpolated between reference points. The interpolated variogram parameters are fed to a locally stationary kriging algorithm that updates the variogram model definition at every estimation point.

Practical Example

The data used for illustrating the proposed approach has been taken from a copper ore deposit drilling database provided with the book “Practical Geostatistics” by S.W. Houlding (2000). For the sake of brevity, only the drill holes north of a transverse fault that divides the deposit in two were considered. For the same reason, the modelling of only the massive black ore (MBO) type, among several others, is presented in this paper. The volume for modelling is a region of 154m x 270m x 226m. For a description of the geology and the drill hole data of this deposit remit to the cited book.

The 2653 2m sample intervals in the northern part of the deposit were coded according the indicator function presented in (1). The proportion of samples intercepting the MBO was calculated as 6.704% after declustering the indicator coded intervals. The distance weights for the calculation of experimental location-dependent indicator correlograms were obtained a Gaussian kernel with 40m bandwidth, which is similar to the separation between drill hole fans. The experimental location-dependent indicator

correlograms were calculated for 9 directions at 168 reference points located in a 40m x 40m grid. The $1-\rho_{VI}(\mathbf{h};\mathbf{o})$ values were used for fitting automatically all variogram model parameters, excepting the shape, which was fixed as exponential, and the dip angle, which was locally conditioned to the bending of the BMO structure in the interpreted sections. Figure 3 shows a representative section with the variogram model parameters for the local plunge angle, and the interpolated local horizontal anisotropy ratios and local vertical anisotropy ratios. The orientation of the maximum horizontal ranges fitted for all experimental local correlograms vary between 170 and 190 degrees azimuth, while a zero nugget effect was obtained at every reference point.

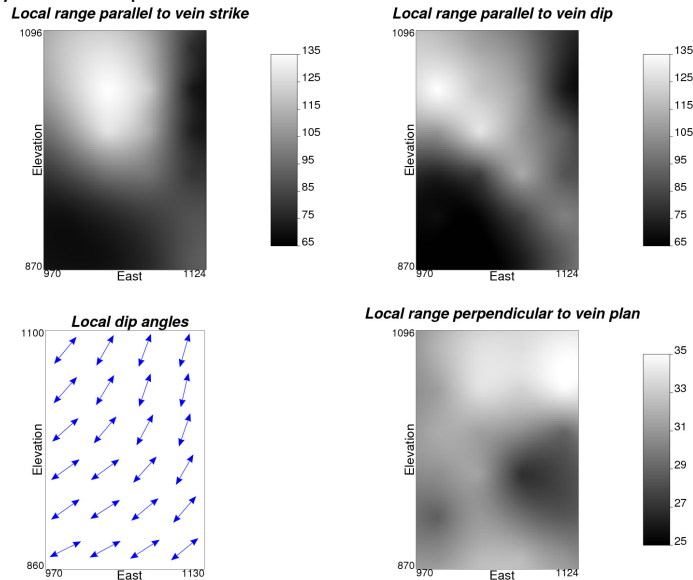


Figure 3: Location-dependent variogram model parameters in a vertical section of the deposit.

The C parameter was fixed as 1 in order to allow a wide uncertainty bandwidth. Different values for the parameter β were tried until finding a close match between the p50 proportion in the interpolated models and the MBO proportion in samples. The value selected was $\beta = 1.55$. Simple Kriging was used for the interpolation of the distance function values. A search sphere with large radius (150m) and a maximum of 96 data points were used for the distance estimation at each node. Using a large number of samples in the distances of interpolation improves the continuity of the resulting vein model, but slows the interpolation. Figure 4 shows a plan and a vertical section of the interpolated distance models and their associated uncertainty bandwidth. This figure is coloured by 1-p values.

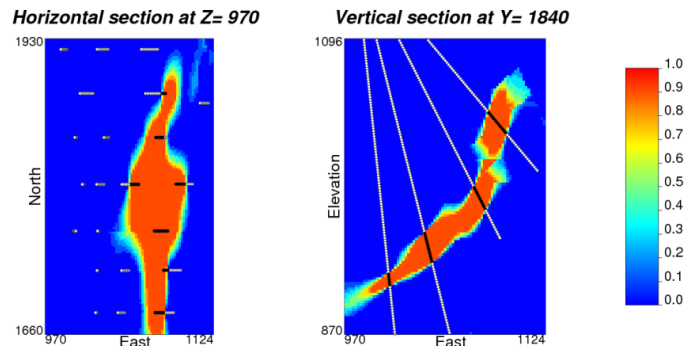


Figure 4: Horizontal (left) and vertical (right) sections showing the uncertainty bandwidth of the ore body model. Higher values indicate a higher probability of being inside the MBO structure.

Error! Reference source not found. shows the distribution of ore body volumes for the entire range of p-values. The deterministic volume calculated from the wireframe model, is for this case, only slightly superior to the p50 volume. The range of volumes obtained using a full uncertainty bandwidth is wide.

The validation of this range of uncertainty can be done by comparing the distance function model with models obtained from stochastic simulation methods.

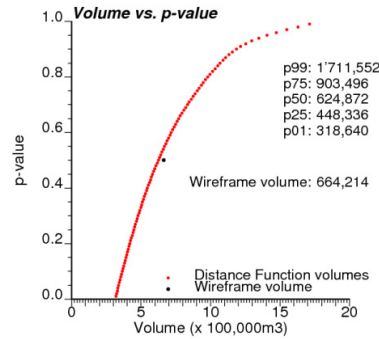


Figure 5: Uncertainty values associated to the range of volumes within the uncertainty bandwidth.

Conclusions

The kriging of distance function values using locally changing variogram model parameters is a more efficient alternative to classic wireframe modelling of ore bodies. The section interpretation stage of the traditional geological modelling methodology is replaced by the modelling of local measures of spatial continuity, which are used for depicting local changes in the vein geometry. Complex ore body geometries can be handled efficiently by the kriging with local parameters algorithm. Additionally a measure of volume uncertainty based in the partial or full calibration of the distance function parameters is provided. Although this is not a rigorously probabilistic approach, it is less demanding than stochastic simulation algorithms. Partial calibration of the DF parameters allows minimizing the bias in the resulting models, while the choice of the parameter controlling the uncertainty bandwidth is left to a reasonable judgement. A full calibration can be performed by optimizing these parameters in relation to equivalent models built by a simulation technique. This leads to consistent parameters in terms of unbiasedness and fair uncertainty but is highly demanding in computational resources. This procedure will be developed in a future work. Other future improvements to the methodology presented in this paper include the use of local drill hole separations, local vein anisotropies, modelling in presence of faults and simultaneous modelling of multiple geological units.

References

- Cowan, E. J., Beatson, R. K., Fright, W. R., McLennan, T. J., & Mitchell, T. J. (2002). Rapid geological modelling. *Applied Structural Geology for Mineral Exploration and Mining, International Symposium*. Kalgoorlie, WA, Australia.
- Cowan, E. J., Beatson, R. K., Ross, H. J., Fright, W. R., McLennan, T. J., Evans, T. R., et al. (2003). Practical Implicit Geological Modelling. In S. Dominy (Ed.), *5th International Mining Geology Conference* (pp. 89-99). Bendigo, Victoria: The Australasian Institute of Mining and Metallurgy.
- Deutsch, C. V., & Journel, A. G. (1998). *GSLIB. Geostatistical software library and user's guide* (2nd Edition ed.). New York: Oxford University Press.
- Gibbs, B. L. (1990, August 1). Mining software trends and applications. *Mining Engineering Magazine*, pp. 974-981.
- Houlding, S. W. (2000). *Practical Geostatistics, Modeling and Spatial Analysis* (1st Edition ed.). Berlin: Springer.
- Machuca-Mory, D. F., & Deutsch, C. V. (2008). Location Dependent Variograms. *Proceedings of the Eighth International Geostatistics Congress, Geostats 2008* (pp. 497-506). Santiago, Chile: GECAMIN Ltd.
- McLennan, J. (2007). *The Decision of Stationarity*. Civil & Environmental Engineering. Edmonton: University of Alberta.
- Munroe, M. J., & Deutsch, C. V. (2008a). A Methodology for Modeling Vein-Type Deposit Tonnage Uncertainty - Paper 301. *Report 10*. Centre for Computational Geostatistics (CCG).
- Munroe, M. J., & Deutsch, C. V. (2008b). Full Calibration of C and Beta in the Framework of Vein-Type Deposit Tonnage Uncertainty - Paper 302. *Report 10*. Centre for Computational Geostatistics (CCG).
- Srivastava, M. R. (2005). Probabilistic Modeling of Ore Lens Geometry: An Alternative to Deterministic Wireframes. *Mathematical Geology*, 37 (5), 513-544.